JMEPEG (2016) 25:2936–2942
DOI: 10.1007/s11665-016-2163-8

1059-9495/$19.00

Morphology and Texture of Zinc Deposits Formed at the Edge of a Rotating Washer Electrode

L.N. Bengoa, P.R. Seré, M.S. Conconi, and W.A. Egli

(Submitted October 13, 2015; in revised form May 20, 2016; published online June 10, 2016)

In this paper, a rotating washer electrode was used to simulate the industrial conditions of strip edges during electrogalvanizing. Using this experimental setup, morphology and texture of the zinc deposits and dendrites formed at the edge of the electrode were studied. Dendrite precursors in the corner of the washer edge were well characterized and their nucleation and growth were also studied. The results indicated that the rotation speed has little effect on texture while, in contrast, current density modifies dendrite's texture. It was found that dendrites are formed by platelets which are stacked on one another, which grow up in a series of steps oriented in the direction of growth of the dendrite's stem yielding highly oriented structure. The presence of sodium ions in the electrolyte changes the morphology and shape of dendrites leading to rounded, 'cabbage'-shaped crystals, while thiourea changes the morphology of both the deposit in the flat portion of the washer and the dendrites through adsorption on the zinc surface.

Keywords crystal orientation, dendritic growth, electroplating, texture, zinc

1. Introduction

Obtaining homogeneous metal electrodeposits on flat surfaces is a relatively simple process. However, when the parts to be covered have intricate shapes (rough or slotted surfaces) some considerations should be taken into account to avoid problems related to current distribution, both primary and secondary (Ref 1, 2). This kind of problems produce areas of low or high current density which lead to the production of heterogeneous or even spread coatings. The latter are generated when the surface has ridges or peaks, i.e., points where the metal is preferentially deposited (high current density) and on which, under certain conditions, dendritic growth occurs (Ref 3, 4). Such growth is usually observed on edges of an electrogalvanized plate, which is obtained by electrodeposition of zinc from an acid sulfate electrolyte. The result of this process is the presence of non-adherent deposits which are easily detached generating quality defects during subsequent forming processes. One possible solution is to determine the values of the operating variables (of the production line) at which dendrite growth can be prevented. The influence of variables affecting the formation of dendrites has been widely studied in recent decades (Ref 4-6), mainly in static conditions with simple geometries that are quite different from those found in industrial lines. Therefore, in order to understand how the process variables influence dendritic growth during electrogalvanization, the rotating washer electrode (RWE) was designed: an electrochemical cell that replicates the fluid dynamics and the current distribution on the sheet edge. Several operating parameters were studied with the RWE in previous works (Ref 7, 8); these results showed that electrolyte flow and current density have a great influence on the kinetics of dendrite growth. Nevertheless, the aforementioned research was focused on the formation of dendrites and little attention was paid to their morphology and texture. As it is known, these properties are modified during zinc electroplating by many parameters such as current density, pH, speed of sheet, electrolyte temperature, and additives addition (Ref 9, 10), affecting the quality and appearance of the coating. All these studies were performed on flat surfaces and have helped to understand how zinc coatings grow. Additionally, different morphologies for zinc deposits were identified and correlated with preferred crystal orientations (Ref 11-14). For example, the ridge morphology (well-aligned tilted hexagonal platelets) is generally associated with a pyramidal non-fiber texture, whereas triangular pyramids appear on the surface when texture is fiber pyramidal (Ref 11). Moreover, some authors even established a relationship between deposit's texture and corrosion resistance (Ref 11, 15), a relevant property of electrodeposited zinc. Thus, since morphology and texture affect deposits properties, it is of interest to determine how these variables affect dendrite's morphology and whether there is any difference with coating's texture. Consequently, in this study the effect of rotational speed and current density on the texture and morphology of dendrites at the edge of steel washers was studied. Also, in some experiments Na^+ was added to the electrolyte and its influence on the morphology of dendrites was characterized.

L.N. Bengoa and **P.R. Seré**, Centro de Investigación y Desarrollo en Tecnología de Pinturas (CIDEPINT), CICPBA-CONICET, Av. 52 e/ 121 y 122, 1900 La Plata, Argentina, and Engineering School, Universidad Nacional de La Plata, Av.1 y 47, 1900 La Plata, Argentina; **M.S. Conconi**, Engineering School, Universidad Nacional de La Plata, Av.1 y 47, 1900 La Plata, Argentina; and Centro de Tecnología de Recursos Minerales y Cerámica (CETMIC), CICPBA-CONICET, Cno. Centenario y 506, 1900 La Plata, Argentina; and **W.A. Egli**, Centro de Investigación y Desarrollo en Tecnología de Pinturas (CIDEPINT), CICPBA-CONICET, Av. 52 e/ 121 y 122, 1900 La Plata, Argentina. Contact e-mails: leandrobengoa@gmail.com and anelpire4@cidepint.gov.ar.

2. Materials and Methods

In order to perform the experiments, a cell specially designed to simulate the current distribution and fluid dynamics

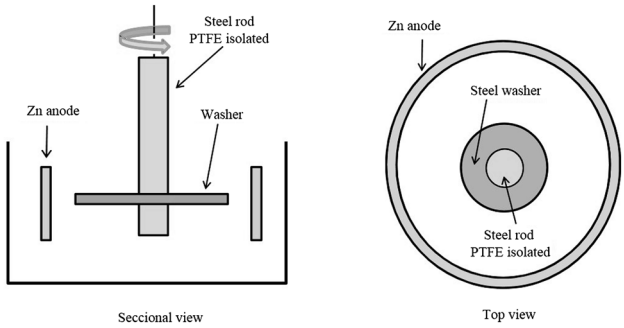

Fig. 1 Schematic representation of the electrochemical cell used in this work (Ref 8)

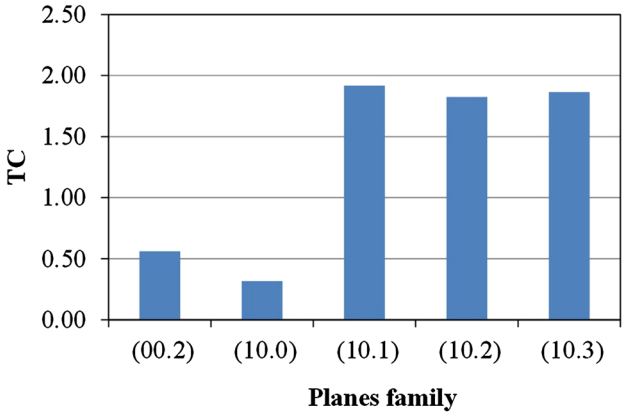

Fig. 2 Texture coefficient on the flat portion of a washer (j = 20 A/dm^2)

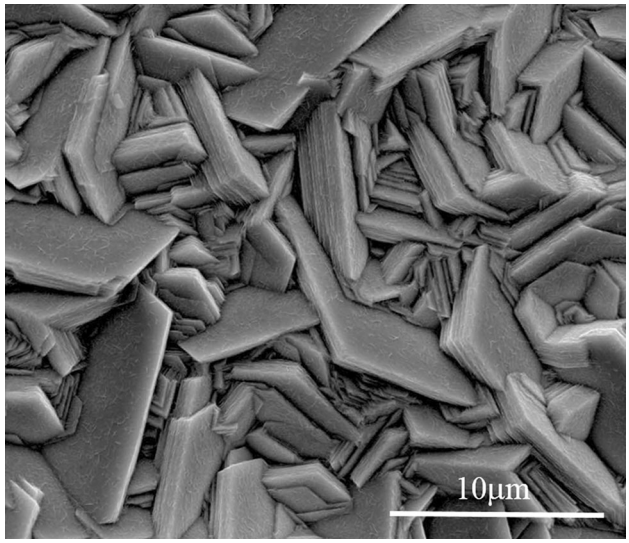

Fig. 3 SEM micrograph of the flat portion of a washer; deposition time t = 180 s (j = 20 A/dm^2)

of the steel strip edge during electrogalvanizing (Ref 7, 8) was used (Fig. 1). Steel washers with an outer diameter of 40 mm and an inner diameter of 8 mm were used as substrates. They were obtained by laser cutting of a 0.7-mm-thick SAE 1010 plate. The washers were mounted on a steel shaft insulated with

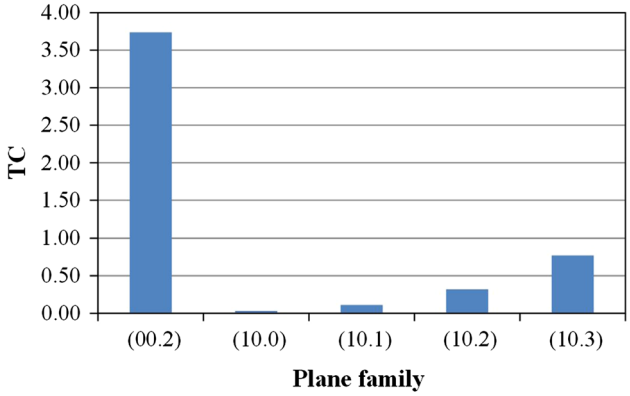

Fig. 4 Texture coefficient on the flat portion of a washer (j = 60 A/dm^2)

PTFE, leaving an exposed area of 0.194 dm^2. A zinc ring with inner diameter 70 mm, obtained by casting from an ingot of pure Zn (99.9%), was used as an anode (0.660 dm^2).

The deposits were obtained from a solution of $ZnSO_4 \cdot 7H_2O$ (Biopack, 99.9%) dissolved in double-distilled water ($[Zn^{2+}]$ = 90 g/L). Its pH value was adjusted to 2 (at 20 °C) by the addition of sulfuric acid (Anedra 98%). In some trials, 18g/L of Na^+ as Na_2SO_4 was added (usually used in industrial lines to improve the electrolyte conductivity). Thiourea, a widely used brightening additive in zinc plating baths, was added (5 g/L) to the electrolyte and its effect on the morphology of the deposit and dendrites was investigated. The deposition temperature was set to 60 °C and it was controlled with a thermostatic bath Frigomix 1495. Zinc deposits were obtained galvanostatically controlling the current with a DC power supply HY3020 FullEnergy. The cathodic current density (j) was varied between 20 and 60 A/dm^2, to match the experimental conditions used in continuous steel strip electrogalvanizing lines. The range of washer rotation speed studied was 400-1200 rpm, chosen to represent the fluid dynamic conditions of the strip edge in the industrial production line. Considering that the electrolyte in the industrial process flows in the opposite direction to the strip and that flow and line speeds are 1 and 0.67 m/s, respectively, the rotation speed was set to achieve a tangential velocity at the washer edge of 1 + 0.67 m/s = 1.67 m/s. This procedure yielded a value of 800 rpm around which the investigation was carried out.

To evaluate the effect of j on the texture and morphology of dendrites, the rotation speed was set to 800 rpm, whereas, to evaluate the effect of the rotational speed, the j used was 40 A/dm^2. Both values correspond to the average of the considered range for each variable. Deposition was carried out during a time far longer than the dendrite induction time (τ) to generate enough samples for XRD measurements. As determined in an earlier study (Ref 8), $\tau \approx$ 17-35 s in all the experimental conditions was considered; thus, the deposition time was fixed at 180 s. Additionally, some deposition experiments were stopped at 5 s ($t << \tau$), 15 s ($t < \tau$), and 40 s ($t > \tau$) to investigate the morphology of dendrite precursors during their initial stage of growth. Since the roughness produced by laser cutting is not representative of those found in industry, the edges of the washers were ground using a systematic procedure (Ref 8). Samples were placed in a rotating system and rotated at 600 rpm. G80 samples were ground using 80-grit sandpaper for 1 min at constant pressure. On the other hand, G600 samples

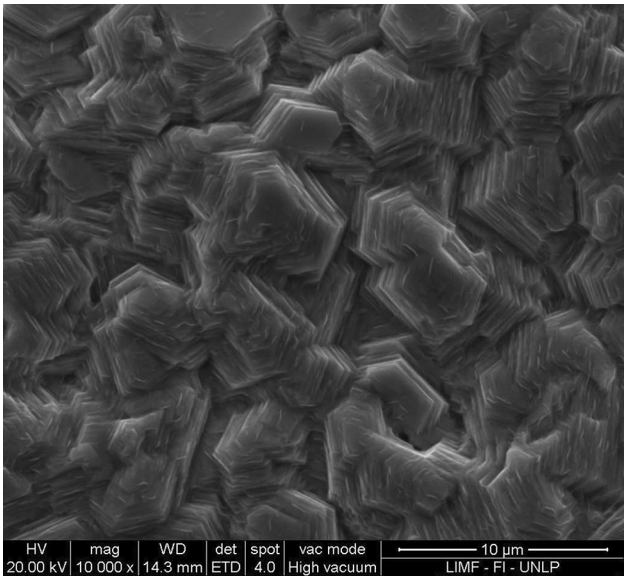

Fig. 5 SEM micrograph of the flat portion of a washer; deposition time t = 180 s (j = 60 A/dm^2)

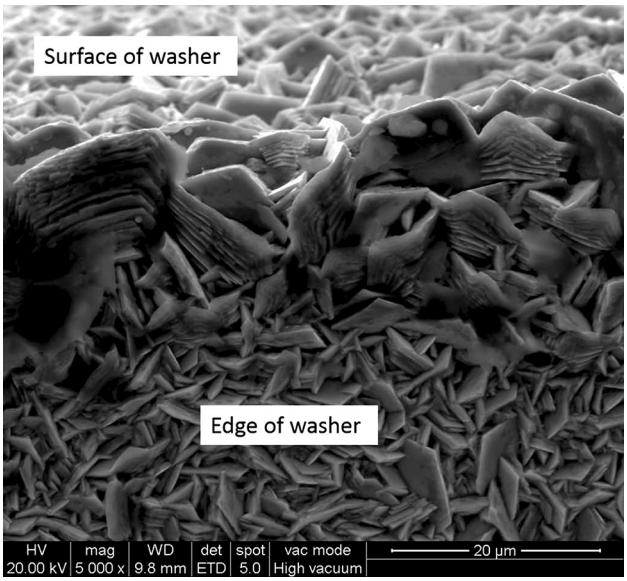

Fig. 6 SEM micrograph showing dendrite formation at the corner of washer edge; deposition time t = 5 s

were ground for 1 min with 180-grit, 1 min with 320-grit, and finally 1 min with 600-grit sandpapers. A hard plastic block was used as a backup for the sandpapers. The finishing procedures were also applied to the flat portion of the washer, onto which the resulting roughness was measured with a profilometer Homer T1000. The results showed that the G80 samples have an average roughness (Ra) of 0.80 µm, while the value for G600 was 0.24 µm. The roughness of industrial sheet is between 0.50 and 1.50 µm meaning that G80 samples are more representative.

Zinc deposits were characterized with scanning electron microscopy (SEM) using a Quanta 200 FEI (tungsten filament) microscope. X-ray spectra (XRD) of dendrites and coatings were determined with a Phillips X'Pert diffractometer with CuKα radiation (1.5405 Å). The scan mode detector with a step

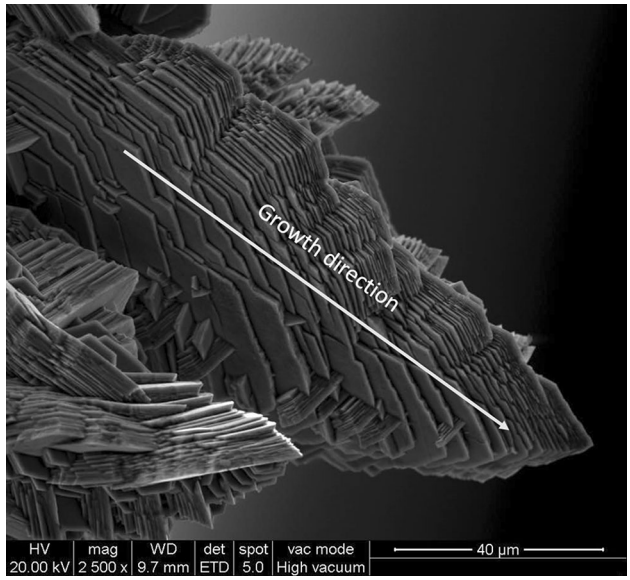

Fig. 7 SEM micrograph showing the growth of a dendrite; deposition time t = 40 s

of 0.05° and a sampling time of 3 s (scan rate 0.0167°/s) was used. The crystallographic orientation was determined through calculation of the texture coefficient ($TC_{(hk.l)}$) using Eq 1:

$$TC_{(hk.l)} = \frac{I_{(hk.l)}}{I_{0(hk.l)}} \frac{1}{\left[\frac{1}{n}\sum \frac{I_{(hk.l)}}{I_{0(hk.l)}}\right]}, \quad \text{(Eq 1)}$$

where $I_{(hk.l)}$ and $I_{0(hk.l)}$ are the intensities corresponding to the planes ($hk.l$) of sample and standard, respectively (ASTM 4-831 chart for a sample of zinc powder), and n is the number of planes in the diffraction pattern. To perform XRD of dendrites, they were placed on an adhesive tape, so that they are located parallel to the surface. Therefore, the crystallographic plane of dendrite growth is perpendicular to the sample surface and is therefore the one that diffracts the least.

Morphology and texture characterization was also performed on the flat portion of the samples to correlate these properties with those of the dendrites.

3. Results and Discussion

Although it is known that edge roughness has a strong effect on the initiation time and propagation rate of dendrites (Ref 7, 8), no influence on the texture and morphology of dendrites was found in the evaluated range (not shown). Therefore, only the results for the samples G80 are presented in the following paragraphs.

Texture coefficient of a zinc coating obtained at 800 rpm and low j located in the flat section of the washer show that it has a great component of pyramidal planes (10.1), (10.2), and (10.3) parallel to the surface and, to a lesser extent, basal planes (00.2) (Fig. 2). This is in agreement with the findings of other authors during deposition from an acid medium under similar conditions (Ref 11, 13, 15). The mainly pyramidal texture generates a surface morphology known as ridge, composed of hexagonal crystals (platelets) inclined with respect to the substrate surface (Fig. 3) (Ref 11). These form parallel ledges, identified as edges

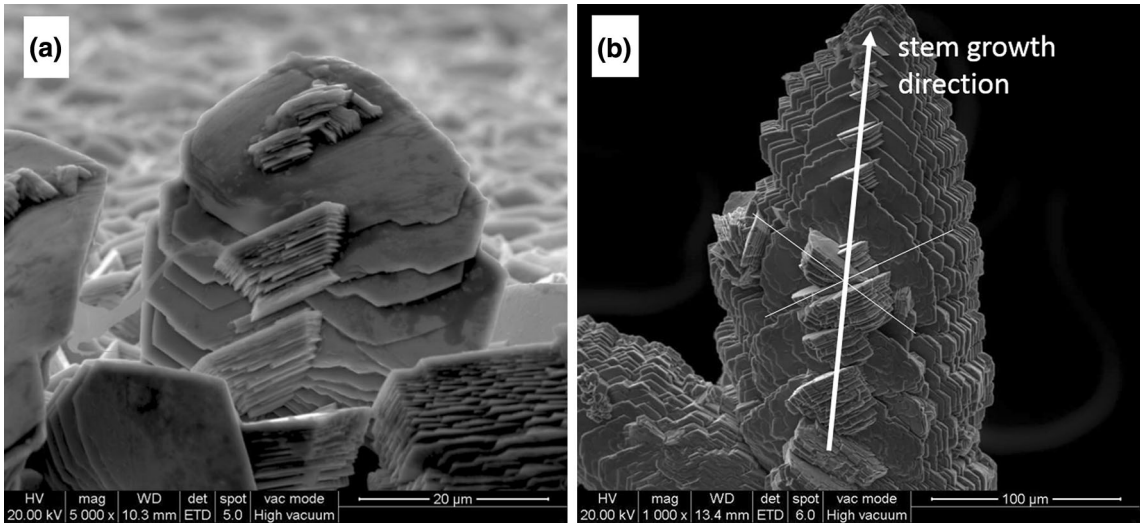

Fig. 8 SEM micrograph showing the (a) nucleation (t = 15 s) and (b) development of new platelets along a dendrite (t = 180 s)

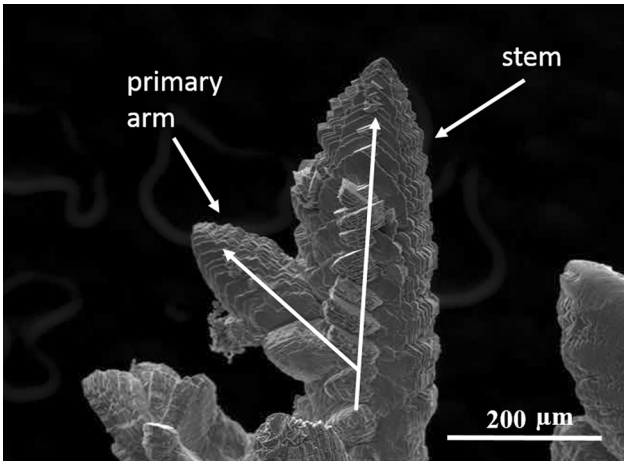

Fig. 9 SEM micrograph showing the formation of primary arms; deposition time t = 180 s

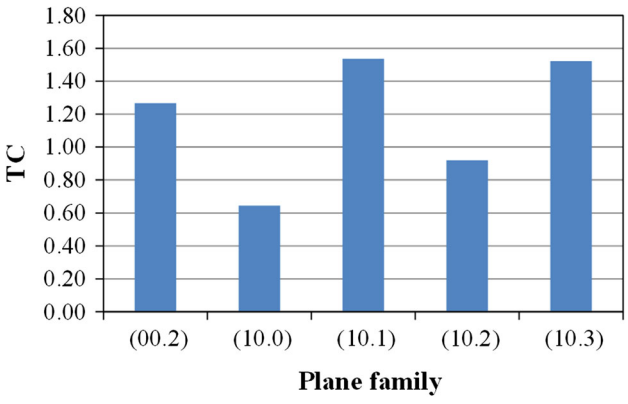

Fig. 10 Texture coefficient of dendrites formed on a washer edge

of the zinc basal plane, which stem from the epitaxial growth of zinc through a 2D nucleation and bunching mechanism. The formation of zinc hydroxide layer on the surface, which is predominant at low overpotentials, is responsible for the development of such microstructures since it inhibits 3D nucleation and the development of basal fiber textures (Ref 12, 16-18). This mechanism plays an important role in crystal growth under industrial conditions (Ref 18). At higher j (60 A/dm^2), an increase of fibber basal texture (00.2) was observed (Fig. 4); this type of texture develops from a 3D nucleation. As the overpotential increases, the adsorption of zinc hydroxide on the surface is inhibited. Under these conditions, a non-epitaxial growth takes place to yield Zn crystals with a shape that minimizes the surface energy of the system. Hence, as the deposit grows, crystal faces with higher energy tend to reduce their surface area, whereas those with lower energy tend to increase it. As a result of this, crystals with higher surface energy are prevented from growing in detriment of those having a lower surface energy (Ref 19, 20). Planes (00.2) are highly compact so crystals with this orientation parallel to the surface will have lower surface energy. Thus, during non-epitaxial growth, where extensive zinc hydroxide adsorption does not occur, a fiber basal texture is expected. The increase in j changes the type of zinc nucleation and, consequently, the texture and morphology of the coating. At high j, the platelets of zinc are located parallel to the surface (Fig. 5).

As regards dendrite formation, under certain conditions of potential or j the presence of small bumps (corner of the washer edge) can promote dendritic growth as a result of concentration of current lines in those points (Ref 1, 21, 22). These structures are highly regular crystals, a characteristic feature of crystal growth under activation control (Ref 7, 23-25). In the j range considered in this work, the dendrites grow with the same morphology of the crystals developed at the surface (Fig. 6), during the first stage of formation. These propagate by the stacking of platelets parallel to each other leading to the development of microscopic steps. The direction of dendrite growth is almost parallel to the platelet, creating what is called the stem of dendrites (Fig. 7). The latter spreads towards the bulk of the solution following the current lines. During its growth, along the length of dendrites new nuclei are continuously formed (Fig. 8a), from where new hexagonal platelets start growing. These also grow by stacking and form angles close to 60° and 120° with respect to the stem of the dendrite (Fig. 8b). Usually, some of these nucleus will thrive, forming

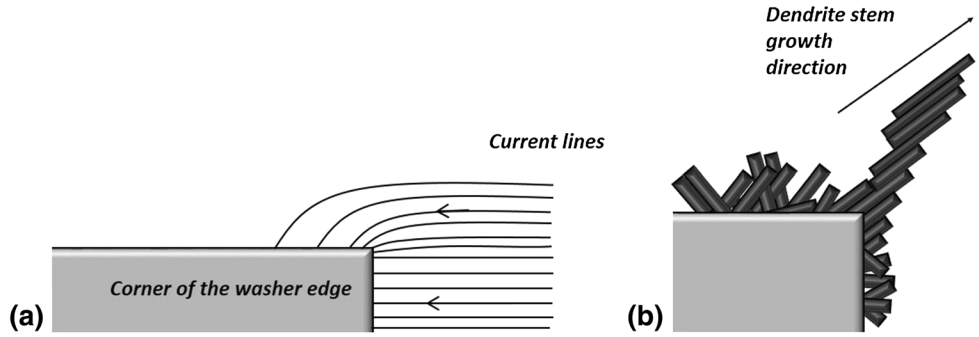

Fig. 11 (a) Current distribution near the corner of the washer's edge; current lines accumulate in the corner. (b) Dendrite stem growing away from the electrode following current line direction

Table 1 TC of dendrites obtained at different speeds of rotation

	Rotation speed, RPM		
Plane	**400**	**800**	**1200**
(00.2)	1.27	1.29	1.25
(10.0)	0.64	0.65	0.87
(10.1)	1.54	1.56	1.34
(10.2)	0.92	0.93	0.96
(10.3)	1.52	1.54	2.01

Table 2 TC of dendrites obtained at different speeds of rotation

	Current density, A/dm^2		
Plane	**20**	**40**	**60**
(00.2)	1.03	1.29	1.43
(10.0)	0.80	0.65	0.76
(10.1)	1.67	1.56	1.38
(10.2)	0.95	0.93	0.81
(10.3)	1.75	1.54	1.19

primary arms like the one shown in Fig. 9. As a result of this growing mechanism, dendrites formed on these samples have a higher prismatic component (10.0) than the flat portion, since this family of planes is the one with the lowest TC value (Fig. 10). This implies that during the dendrite development, the growth direction is perpendicular to the (10.0) plane and parallel to the basal plane. As mentioned before, dendrites begin to grow with the same morphology as that observed in the flat surface. However, during its development the platelets grow on one another trying to spread out in the direction of current lines (Fig. 11). Consequently, platelet centers are not aligned which leads to the formation of macrosteps (built by multiple atomic layers). The growth direction of dendrite stem is contained in the basal plane (face of platelets), and thus a prismatic texture develops.

Experiments carried out at different rotation speeds showed that this variable has no influence on the TC of either the deposit on the flat portion of the washer or the dendrites formed at washer edges. Samples obtained at the speeds of 400, 800, and 1200 rpm presented similar TC values (Table 1). In contrast, j induced changes in TC of dendrites. While TC remained predominantly prismatic, increasing j leads to a decrease of the basal texture and increased pyramidal texture (Table 2). None of these variables caused significant changes in the morphology of neither the flat portion nor the dendrites.

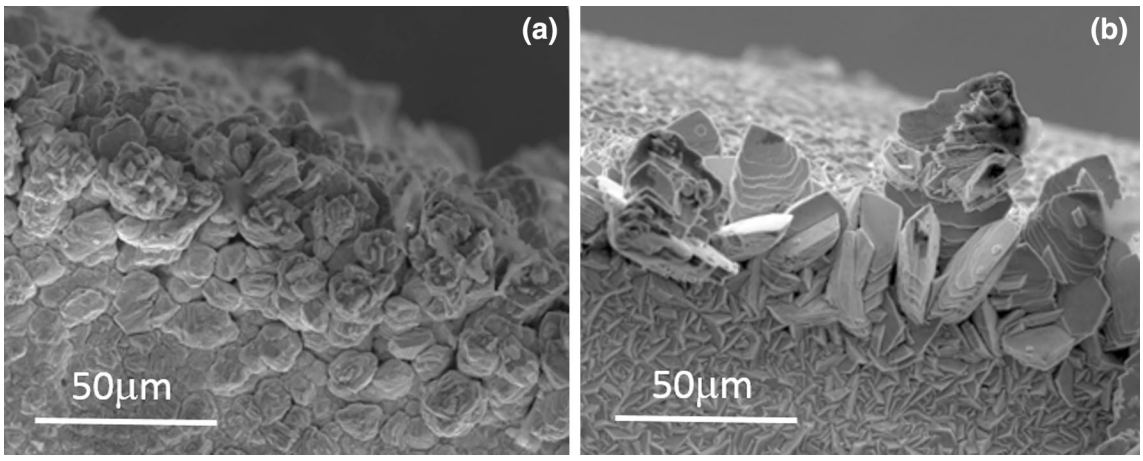

Fig. 12 SEM micrograph showing dendrite formation at the corner of washer edge: (a) with Na^+ and (b) without Na^+. Deposits were obtained at 40 A/dm^2 and 800 rpm (t = 20 s)

The addition of Na_2SO_4 to the electrolyte reduced the size (Fig. 12) and changed the morphology of dendrites, although the deposit on the flat portion was barely modified (800 rpm and 60 A/dm^2). This is probably because sodium ions do not take part in the zinc deposition mechanism, thus not affecting the nucleation and growth process. Nevertheless, Na^+ leads to an increase in the specific conductivity of the electrolyte from 96 mS/cm without Na^+ to 125 mS/cm with the addition of 18 g/L of Na^+. This improves the current distribution on the edge of the washer reducing significantly the size of the dendrites (Ref 7). The improvement in the current distribution causes the current flow in the edge of washer to be less directional. Therefore, zinc crystals are grouped more randomly, acquiring rounded shapes, such as cabbages (Fig. 12a). As regards crystal orientation, it was found that the presence of Na^+ in the solution causes no changes in the TC values of the flat portion. These measurements could not be performed on dendrites due to their round shape. When they were detached from the substrate, it was impossible to align them in their growth direction (see section 2).

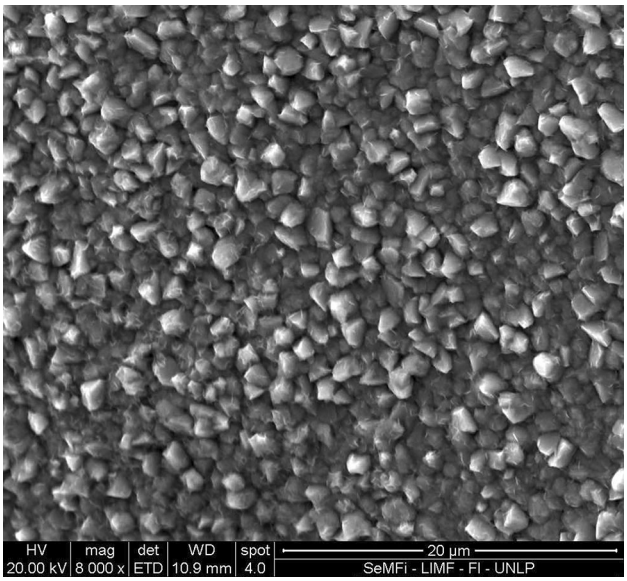

Fig. 13 SEM micrograph of the flat portion of a Zn deposit obtained in the presence of thiourea (5 g/L); deposition time t = 180 s (j = 60 A/dm^2)

Finally, thiourea was added to the electrolyte and deposits were obtained at high j (60 A/dm^2). Figure 13 clearly shows that this additive induces a change in the morphology of the flat portion of the deposit (see Fig. 3). In this case, small pyramids appear on the coating surface, which result from a preferential growth of zinc crystals in the direction of the pyramidal planes (10.1), (10.2), and (10.3). The latter was further confirmed by XRD measurements which show that in the presence of thiourea the TC values of these planes are at least two times higher than those in its absence. A possible cause of these changes is the preferential adsorption of thiourea on basal planes increasing their surface energy and, therefore, hindering their growth and changing the crystal habit (Ref 26-28). Grain refinement is also induced by this additive as seen in Fig. 13, which stems from the inhibition of crystal growth aforementioned. In agreement with the discussion in previous paragraphs, a change in the morphology of the deposit leads to changes in the morphology of dendrites (Fig. 14). Since thiourea induces the development of a pyramidal texture, dendrites are similar to those obtained at low j in the absence of this additive.

With regard to dendrite growth, it was found that thiourea reduces the size of dendrites. This is not a surprising result since thiourea is commonly used as a brightening additive for acid zinc plating solutions. Generally, organic compounds adsorb to a larger extent at high-j zones, such as peaks, improving the current distribution at the electrode (Ref 29).

4. Conclusion

Dendritic structure is highly regular, which is a characteristic feature of crystal growth under activation control. These grow by the stacking of hexagonal platelets which develop parallel to each other forming steps which are oriented in the direction of growth of the dendrite stem. It was found that dendrites formed in the corner of the washer edge have higher

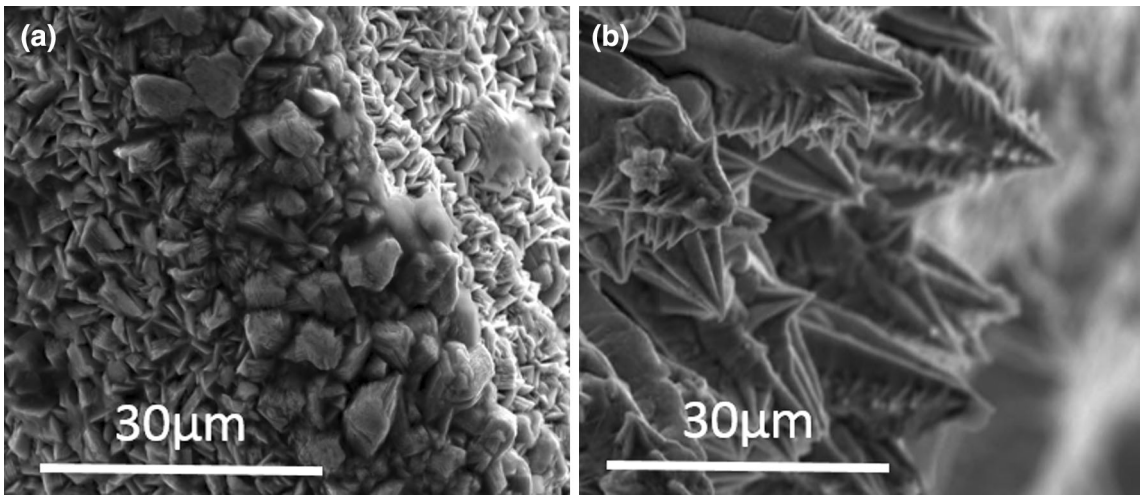

Fig. 14 SEM micrograph showing dendrite formation at the corner of washer edge: (a) with 5 g/L thiourea and (b) without additives. Deposits were obtained at 60 A/dm^2 and 800 rpm (t = 5 s)

prismatic component than the flat portion thereof. Regarding the effect of operating conditions, it can be concluded that the variation of rotation speed has a negligible effect on crystal orientation, while current density modifies dendrite's texture. However, none of these induce significant changes in the morphology of dendrites. In contrast, addition of Na^+ to the bath, modifying its conductivity but not the nucleation and growth mechanism, induces considerable modification in dendrite's morphology but not in the flat portion of deposit. Thiourea strongly adsorbs on zinc and modifies the deposition mechanism so the morphologies of both the deposit and the dendrites are changed by its presence in the solution.

Acknowledgments

The authors would like to acknowledge the Comisión de Investigaciones Científicas de la Provincia de Buenos Aires (CICPBA), Consejo Nacional de Investigaciones Científicas y Técnicas (CONICET), and Universidad Nacional de La Plata (UNLP) for their financial support to this work.

References

1. N. Ibl, *Current Distribution, Comprehensive Treatise of Electrochemistry*, Plenum Press, New York, 1983, p 239–311
2. J.S. Newman, *Applications of Potential Theory, Electrochemical Systems*, Prentice Hall Inc., New Jersey, 1991, p 378–396
3. K.I. Popov and N.D. Nikolic, General Theory of Disperse Metal Electrodeposits Formation, *Electrochemical Production of Metal Powders*, S.S. Djokić, Ed., Springer, New York, 2012, p 1–62
4. K.I. Popov, M.G. Pavlovic, and M.D. Maksimovic, Comparison of the Critical Conditions for Initiation of Dendritic Growth and Powder Formation in Potentiostatic and Galvanostatic Copper Electrodeposition, *J. Appl. Electrochem.*, 1982, **12**, p 525–531
5. G. Wranglén, Dendrites and Growth Layers in the Electrocrystallization of Metals, *Electrochim. Acta*, 1960, **2**, p 130–146
6. J.W. Diggle, A.R. Despić, and J.O.M. Bockris, The Mechanism of the Dendritic Electrocrystallization of Zinc, *J. Electrochem. Soc.*, 1969, **116**(11), p 1503–1514
7. L.N. Bengoa, S. Bruno, H.A. Lazzarino, P.R. Seré, and W.A. Egli, Dendritic Zinc Growth on the Edges of Flat Steel Strip During Electro Galvanizing, *Proc. Mater. Sci.*, 2015, **8**, p 1174–1183
8. L.N. Bengoa, S. Bruno, H.A. Lazzarino, P.R. Seré, and W.A. Egli, Study of Dendritic Growth of Zinc Crystals on the Edges of Steel Sheet, *J. Appl. Electrochem.*, 2014, **44**(12), p 1261–1269
9. Y.B. Yim, W.S. Hwang, and S.K. Hwang, Crystallographic Texture and Microstructure of Electrogalvanized Layer in Acid Sulfate Solution, *J. Electrochem. Soc.*, 1995, **142**(8), p 2604–2611
10. D. Vasilakopoulos, M. Bouroushian, and N. Spyrellis, Texture and Morphology of Zinc Electrodeposited from an Acid Sulfate Bath, *Trans. Inst. Met. Finish.*, 2001, **79**, p 107–111
11. H. Park and J.A. Szpunar, The Role of Texture and Morphology in Optimizing the Corrosion Resistance of Zinc-Based Electrogalvanized Coatings, *Corros. Sci.*, 1998, **40**(4-5), p 525–545
12. K. Raeissi, A. Saatchi, M.A. Golozar, and J.A. Szpunar, Texture and Surface Morphology in Zinc Electrodeposits, *J. Appl. Electrochem.*, 2004, **34**(12), p 1249–1258
13. K. Raeissi, A. Saatchi, M.A. Golozar, and J.A. Szpunar, Effect of Surface Preparation on Zinc Electrodeposited Texture, *Surf. Coat. Technol.*, 2005, **197**(2-3), p 229–237
14. T. Watanabe, *Chapter 7—Database for the Microstructure of Plated Films, Nano Plating—Microstructure Formation Theory of Plated Films and a Database of Plated Films*, Elsevier, Oxford, 2004, p 255–696
15. S.H. Hong, J.B. Kim, and S.K. Lee, The Role of Textures in the Corrosion Resistance of Electrogalvanized Zinc Coatings, *Mater. Sci. Forum*, 2002, **408-412**, p 1025–1030
16. K.R. Baldwin, C.J.E. Smith, and M.J. Robinson, Study Into the Electrodeposition Mechanisms of Zinc-Nickel Alloys from an Acid-Sulphate Bath, *Trans. Inst. Met. Finish.*, 1994, **72**(2), p 79–88
17. T. Tsuru, S. Kobayashi, T. Akiyama, H. Fukushima, S.K. Gogia, and R. Kammel, Electrodeposition Behaviour of Zinc-Iron Group Metal Alloys from a Methanol Bath, *J. Appl. Electrochem.*, 1997, **27**(2), p 209–214
18. G. Xun-lei, S. Yu-qiao, L. Jing, and L. Chang-sheng, Morphology and Texture of High Speed Galvanized Coatings on Interstitial Free Steel Sheet, *Trans. Nonferrous Met. Soc. China*, 2011, **21**, p 488–492
19. D.Y. Li and J.A. Szpunar, Texture Competition in Solidification Process, *Mater. Sci. Forum*, 1994, **157-162**, p 547–554
20. D.Y. Li, J.A. Szpunar, and A. Monte, Carlo Simulation Approach to the Texture Formation During Electrodeposition—II. Simulation and Experiment, *Electrochim. Acta*, 1997, **42**(1), p 47–60
21. A.R. Despić and K.I. Popov, Transport Control Deposition and Dissolution of Metals, *Modern Aspects of Electrochemistry*, B.E. Conway and J.O.M. Bockris, Ed., Butterworths, London, 1972, p 304–310
22. K.I. Popov, S.S. Djokić, and B.N. Grgur, *Surface Morphology of Metal Electrodeposits, Fundamental Aspects of Electrometallurgy*, Kluwer Academic, New York, 2002, p 29–100
23. N.D. Nikolić, K.I. Popov, P.M. Živković, and G. Branković, A New Insight into the Mechanism of Lead Electrodeposition: Ohmic-Diffusion Control of the Electrodeposition Process, *J. Electroanal. Chem.*, 2013, **691**, p 66–76
24. N.D. Nikolić, G. Branković, and U.Č. Lačnjevac, Formation of Two-Dimensional (2D) Lead Dendrites by Application of Different Regimes of Electrolysis, *J. Solid State Electrochem.*, 2012, **16**, p 2121–2126
25. V.D. Jović, N.D. Nikolić, U.Č. Lačnjevac, B.M. Jović, and K.I. Popov, Electrochemical Production of Metal Powders, *Morphology of Different Electrodeposited Pure Metal Powders*, S.S. Djokić, Ed., Springer, New York, 2012, p 63–123
26. L. Oniciu and L. Mureşan, Some Fundamental Aspects of Levelling and Brightening in Metal Electrodeposition, *J. Appl. Electrochem.*, 1991, **21**(7), p 565–574
27. A. Milchev, *Thermodynamics of Electrochemical Nucleation, Electrocrystallization: Fundamentals of Nucleation and Growth*, Springer, Boston, 2002, p 1–82
28. J.W. Mullin, *Crystal Growth, Crystallization (Fourth Edition)*, Butterworth-Heinemann, Oxford, 2001, p 216–288
29. M. Paunovic and M. Schlesinger, *Effect of Additives, Fundamentals of Electrochemical Deposition*, Wiley, New York, 2006, p 177–198